

Cite this: *Nanoscale*, 2011, **3**, 258

www.rsc.org/nanoscale

PAPER

A highly sensitive ultraviolet sensor based on a facile *in situ* solution-grown ZnO nanorod/graphene heterostructure†

Haixin Chang,^a Zhenhua Sun,^b Keith Yat-Fung Ho,^c Xiaoming Tao,^a Feng Yan,^{*b} Wai-Ming Kwok^{*c} and Zijian Zheng^{*a}

Received 12th August 2010, Accepted 14th September 2010

DOI: 10.1039/c0nr00588f

The weak photon absorption and fast carrier kinetics of graphene limit its application in photodetection. This limitation can be overcome by introducing photosensitive nanostructures to graphene. Herein we report the synthesis of a ZnO nanorod/graphene heterostructure by a facile *in situ* solution growth method. By combining the attributes of photosensitive ZnO nanorods and highly conductive graphene, we for the first time demonstrate a highly sensitive visible-blind ultraviolet (UV) sensor based on graphene related heterostructure. The photoresponsibility of the UV sensor can reach 22.7 A W^{-1} , which is over 45,000 fold higher than that of single graphene sheet based photodetectors.

1. Introduction

Graphene is a novel carbon nanomaterial with a unique two-dimensional conjugated structure and electronic properties, and has been intensively studied for applications in electronic devices, nanocomposites, solar cells and sensors.^{1–17} Very recently, a rapidly increasing interest has been focused on graphene based photodetectors. For example, an all-spectrum ultrafast photodetector was developed from mechanically exfoliated single layer graphene, while the photoresponsibility was only limited to $0.1\text{--}0.5 \text{ mA W}^{-1}$ because of the weak light absorption and fast charge carrier kinetics of graphene.¹⁸ To increase the photosensitivity, photo-sensitive nanomaterials such as quantum dots (QDs) or nanoparticles were introduced to graphene to form functional composite materials.^{10,19,20} For instance, we have demonstrated that *in situ* grown CdS QD/graphene heterostructures could work as efficient photoelectrochemical cells which had a high on-

off optical switch.¹⁰ Geng *et al.* prepared non-covalently linked CdSe QD/graphene hybrids that exhibited rapid photo-responsive properties.²⁰ All these graphene based heterostructures or composites were developed for the detection of visible light. However, to the best of our knowledge, no work is reported on the detection of ultraviolet (UV) light with graphene based heterostructures or composites to date, although UV sensors are highly desirable in many fields such as flame detection, environmental studies, medical and communication equipment.^{21,22}

Herein, we demonstrate for the first time the development of visible-blind, UV sensors on the basis of thin films of ZnO nanorod/graphene heterostructures, which are synthesized by a facile *in situ* aqueous seeded growth method. Because of the wide bandgap ($\sim 3.37 \text{ eV}$), ZnO nanostructures are ideal UV-sensitive semiconductors for optoelectronic applications.^{23–27} In the heterostructure reported here, ZnO nanorods function as UV absorbing and charge carrier generating materials, while graphene obtained by chemical reduction of graphene oxide is used as a charge transporting, highly conductive matrix. The photoresponsibility of the as-made UV sensor can reach 22.7 A W^{-1} at 20 V bias, which is over 45,000 folds higher than that of single graphene sheet based photodetectors ($\sim 0.1\text{--}0.5 \text{ mA W}^{-1}$).¹⁸ More importantly, our device shows little response to visible light, critical for sensitive and selective UV sensors.

2. Results and discussion

2.1 Preparation of ZnO nanorod/graphene heterostructure

Fig. 1 shows a schematic illustration of the fabrication of ZnO nanorod/graphene heterostructures. Firstly, highly water soluble, chemically derived graphene was synthesized by a method we developed previously.²⁸ In the meantime, ZnO QDs were synthesized by a non-aqueous method in methanol. The

^aNanotechnology Center, Institute of Textiles and Clothing, The Hong Kong Polytechnic University, Hung Hom, Kowloon, Hong Kong SAR. E-mail: tczzheng@inet.polyu.edu.hk

^bDepartment of Applied Physics, The Hong Kong Polytechnic University, Hung Hom, Kowloon, Hong Kong SAR. E-mail: apafyan@polyu.edu.hk

^cDepartment of Applied Biology and Chemical Technology, The Hong Kong Polytechnic University, Hung Hom, Kowloon, Hong Kong SAR. E-mail: bcwmkwok@inet.polyu.edu.hk

† Electronic supplementary information (ESI) available: A TEM image of ZnO QDs. UV-Vis spectra of ZnO QDs, graphene and ZnO QD/graphene hybrid in methanol–water solution and ZnO nanorods on quartz substrates. *I–V* curves for ZnO QD/graphene hybrid under dark and 590 nm photon radiation. *I–V* curves for SDBS-graphene film under dark and 590 nm photon radiation. Time-resolved photoresponses of the ZnO nanorod/graphene heterostructure, ZnO QD/graphene hybrid and pure SDBS-graphene. Time-resolved photoresponses and photocurrent decay of the ZnO nanorod/graphene heterostructure. SEM image of the ZnO nanorod/graphene heterostructure device after irradiated with long term UV light. See DOI: 10.1039/c0nr00588f

graphene was then mixed with ZnO QDs in a certain ratio to form a mixture solution, which is subsequently cast onto different substrates including glass, quartz, SiO₂/n-Si and polyethylene terephthalate (PET), to yield thin films of ZnO QD/graphene. The films were annealed at a low temperature (100 °C) to evaporate the water and to enhance the adhesion to substrates. The sample was then immersed in a zinc nitrate solution for *in situ* growth of ZnO nanorods from the ZnO QD seeds to yield the ZnO nanorod/graphene heterostructures (Fig. 1A). Finally, the sample was rinsed extensively with water several times to get rid of the loosely attached ZnO nanorods. For UV sensor fabrication, gold electrodes with 100 μm channel length were patterned onto ZnO QD/graphene before the *in situ* hydrothermal growth of ZnO nanorods (Fig. 1B).

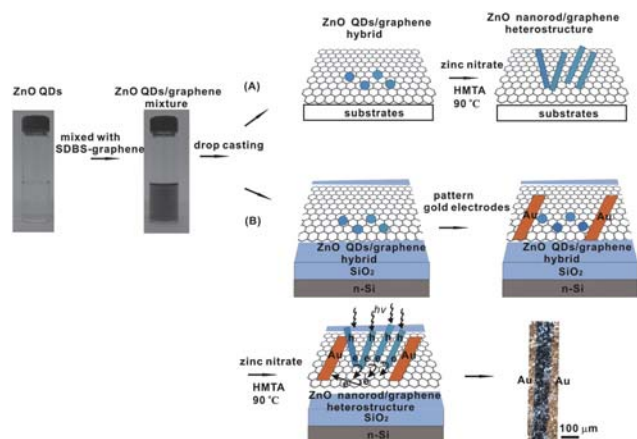


Fig. 1 Schemes for facile synthesis of ZnO nanorod/graphene heterostructures from solution processable ZnO QD/graphene hybrid (A) on various substrates and (B) on SiO₂/n-Si substrate for thin film optoelectronic devices. Upon irradiation with ultraviolet photons, photo-generated electrons will be transported from ZnO nanorods to graphene and further transported to electrodes by graphene with high efficiency. Therefore the ZnO nanorod/graphene heterostructure here can work as a prototype ultraviolet sensor.

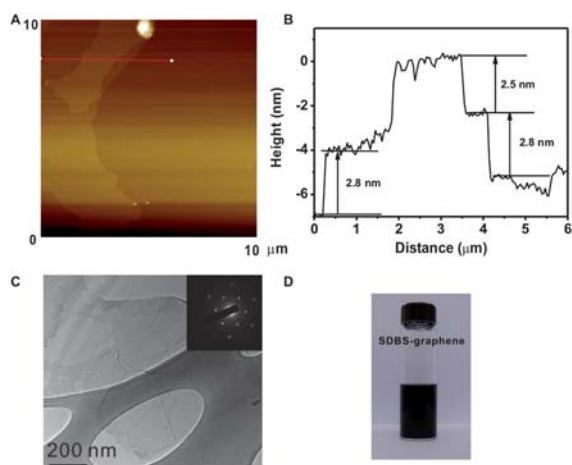


Fig. 2 Tapping mode AFM image (A) and depth profile (B) of SDBS-graphene on Si substrate; (C) TEM micrograph and electron diffraction pattern (Inset) of SDBS-graphene; (D) digital image of 1 mg mL⁻¹ SDBS-graphene aqueous solution.

For facile device fabrication and application purposes, it is very important to obtain highly soluble and large size graphene. In our synthetic strategy, graphite oxide was exfoliated and reduced at the presence of sodium dodecylbenzene sulfonate (SDBS) into chemically reduced graphene (SDBS-graphene).²⁸ The single layer SDBS-graphene is typically ~10 μm in size, and thicker than the mechanically exfoliated one due to the absorption of SDBS (Fig. 2A).²⁸ Measured by tapping mode atomic force microscopy (AFM), single layer and bilayer SDBS-graphene are *ca.* 2.5 and 5.3 nm thick, respectively (Fig. 2B). Transmission electron microscopy (TEM) and its diffraction analysis (Fig. 2C) confirms the high-quality monolayer structure in most of our samples.²⁹ Importantly, the SDBS-graphene can be readily dissolved in water because of the electrostatic charges on the graphene surface induced by SDBS, to form an aqueous solution as concentrated as 1 mg mL⁻¹ (Fig. 2D).^{28,30,31}

The SDBS-graphene was mixed with ZnO QDs in a weight ratio of 1.5 (ZnO to SDBS-graphene) in a methanol–water mixture to yield a grey color solution. The ZnO QDs prepared by non-aqueous method have diameters of 5–10 nm with a lattice spacing of 0.286 nm (Fig. S1, ESI†).³² The mixture was centrifuged and washed several cycles to remove the excess amount of ZnO QDs. TEM images show that ZnO QDs are indeed

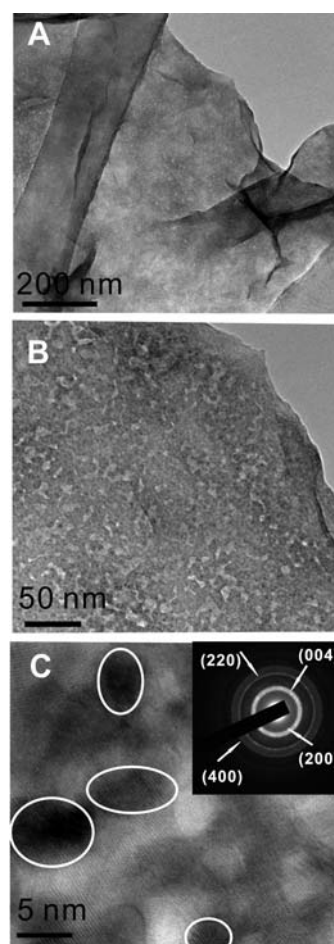


Fig. 3 TEM micrograph of ZnO QD/graphene hybrid at low resolution (A, B) and high resolution (C), inset, electron diffraction of ZnO QDs on graphene.

uniformly dispersed on the SDBS-graphene surfaces, and few free ZnO QDs is found (Fig. 3A–3C). The diffraction pattern of ZnO QDs on graphene further shows a crystal structure of ZnO QDs (inset in Fig. 3C).³³ The fact that ZnO QD/graphene hybrids can be well-preserved after extensive rinsing and centrifuge indicates a strong binding between the ZnO QDs and SDBS-graphene. Considering that the preparation conditions are mild and both the ZnO QDs and SDBS-graphene are negatively charged, we believe that the strong binding force should be attributed to hydrogen bonds and van der Waals interactions. We also believe that the hybrid formation is assisted by the highly wrinkled nature and great flexibility of graphene (due to its two-dimensional sheet structure with one-atom thickness) so that conformal contact between ZnO QDs and SDBS-graphene can be readily made. The ZnO QD/graphene hybrid has a broad UV-vis absorption ranging from 225 nm to 550 nm, in which the 320 nm shoulder peak is attributed to the adsorption of ZnO QDs while the rest of the majority is attributed to the adsorption of SDBS-graphene (Fig. S2A†).

ZnO QD/graphene hybrid film was readily made by casting the mixing solution onto substrates by methods including drop-casting, spincoating, and dip-coating. Typically, we found spincoating and dip-coating of ZnO QD/graphene end up with very thin films of poor coverage of the substrate. Therefore, we adopted drop-casting technique to generate hybrid thin films of ten to several tens of nanometres thick to ensure the formation of a continuous film over 100 μm , which is the distance between gold electrodes of UV sensor as discussed below. The as-made hybrid film is very rough and has many wrinkles through all the surfaces (Fig. 4A and 4B). The thin films were then annealed at 100 $^{\circ}\text{C}$ in an oven for ~ 30 min to evaporate the solvent and to enhance the adhesion to the substrates. Note that this step is critical to prevent the scaling of hybrid films from the substrates, which ensure success of the subsequent growth of ZnO nanorods.

ZnO nanorods can grow *in situ* from ZnO QDs of the hybrid to form ZnO nanorod/graphene heterostructures.³⁴ As a proof-of-concept, the ZnO QD/graphene coated substrate was immersed in an aqueous solution containing 0.025 M $\text{Zn}(\text{NO}_3)_2$ and 0.025 M hexamethylenetetramine (HMTA) at 90 $^{\circ}\text{C}$ for 1 h. Because of the wrinkled and rough morphology of the hybrid template, ZnO nanorods grew upward to all the directions (Fig. 4C and 4D). The ZnO nanorods have a diameter of 50–200 nm and length of 500 nm–1 μm . High resolution scanning electron microscopy (SEM) image shows an enlarged single ZnO nanorod with hexagonal section morphology, indicating a good degree of crystallization of the nanorods (inset in Fig. 4D). TEM microscopy further confirm that the ZnO nanorods are single crystals and they grow along the *c*-axis with a lattice spacing of 0.525 nm (Fig. 4E and 4F), typical of single crystal ZnO nanorods.³⁵ We observe some random ZnO nanorods on top of substrate surfaces that are not covered with ZnO QD/graphene. We believe that it is induced by some residue ZnO QDs on the substrate which initiates the ZnO nanorods growth. We also observe that the ZnO nanorods only grow from the top layer of the hybrid film. Considering of a large amount of ZnO QDs embedded in the hybrid film, a possible explanation is that the hybrid film becomes highly compact after thermal annealing, and the surface growth of ZnO nanorods suppresses the diffusion of Zn^{2+} and HMTA into the inner layers.³⁴ Importantly, the ZnO nanorods

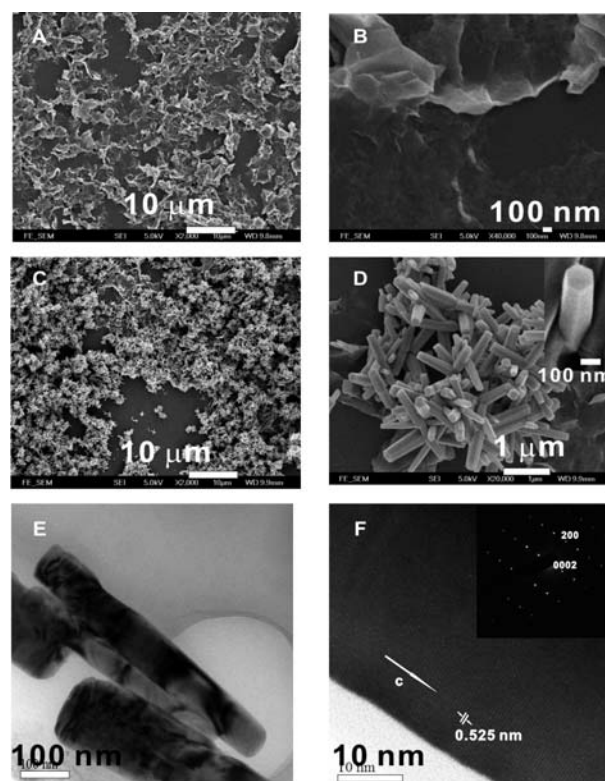


Fig. 4 Low (A) and high (B) resolution SEM micrographs of ZnO QD/graphene hybrid film; low (C) and high (D) resolution SEM micrographs of ZnO nanorod/graphene heterostructure; low (E) and high (F) resolution TEM micrographs of ZnO nanorods, inset of (F), electron diffraction pattern of a single ZnO nanorod.

have a strong absorption ranging from 305 nm to 375 nm with a peak centered at 350 nm (Fig. S2B†). Compared with ZnO QDs, such a red shift in absorption is more desirable for applications as near UV sensors. More importantly, the absorption at visible light regime is much lower than that at UV regime, indicating that the heterostructure should have high selectivity in the photoresponsibility of the UV regime.

2.2 Fabrication and performance of ZnO nanorod/graphene UV sensor

The heterostructure is ideal for use as the active layer in visible-blind, UV sensitive photodetectors. Therefore, we tested the hypothesis by fabricating ZnO nanorod/graphene based sensors using a photoconductor configuration, in which the substrate was $\text{SiO}_2/\text{n-Si}$, and the electrodes were gold. Typically, the ZnO QD/graphene hybrid film was prepared on $\text{SiO}_2/\text{n-Si}$ substrates by the above procedures, followed by thermal evaporation of gold through a patterned mask to generate patterned gold electrodes of 100 μm long and 2 mm wide (Fig. 1B). The ZnO nanorod/graphene heterostructure was then formed in the channels by *in situ* seeded growth method described above. As a proof-of-concept, we use the as-made optoelectronic device to detect 370 nm light by exposing the device under control light intensity while recording the output current (*I*) of the gold electrodes. In a typical experiment, *I* was recorded to be ~ 300 μA at 20 V bias when the device was not irradiated with the UV light.

Upon radiation, I increased monotonically as the 370 nm light power was raised from 0 to 1.084 mW cm^{-2} (Fig. 5A and 5B). For example, I increased by $16 \mu\text{A}$ and $52.7 \mu\text{A}$ at 20 V bias when the UV light power are $65.2 \mu\text{W cm}^{-2}$ and 1.084 mW cm^{-2} , respectively. The UV sensor can achieve 6–7 folds higher photocurrent (both in 20 V and $\sim 0.8 \text{ mW cm}^{-2}$ radiation) than almost the best pure ZnO nanomaterials based traditional metal-semiconductor-metal photodetectors.³⁶ The current increase can be explained by the addition of photogenerated electrons from ZnO nanorods and efficient charge collection and transport of graphene. When the ZnO nanorods are irradiated with UV light, hole and electron pairs will be generated. Because ZnO is an electron transporting material, photogenerated electrons can readily flow into the SDBS-graphene through graphene/ZnO junctions. The SDBS-graphene can then transport the photogenerated charge carriers effectively to the gold electrodes because of its high electronic mobility and conductivity.^{10,19,20} As a result, a net increase in the output current is recorded.

Having proven that the ZnO nanorod/graphene heterostructure is highly responsive to 370 nm UV light, we then systematically examined the device performance. The amount of current increase under radiation (compared with the current in dark at 20 V) is plotted against the power of the incident UV light. This calibration curve shows a strong linear relationship with a linear coefficient $R^2 = 0.99$ (Fig. 5C), indicating that our ZnO nanorod/graphene based optoelectronic device can potentially be utilized as a quantitative UV sensor. Importantly, the device does not have photoresponse to visible 590 nm light, which is attributed to the wide energy bandgap in ZnO so that no carrier is excited at low-energy visible photons (Fig. 5D). This characteristic is critical to the applications in highly selective visible-blind UV sensors. The device achieves as high as 22.7 A W^{-1} efficiency at 20 V bias, over 45000 folds higher than that of single layer graphene photodetectors ($\sim 0.1\text{--}0.5 \text{ mA W}^{-1}$).¹⁸ Compared

with photodetector using pure ZnO nanostructures as the active layer (which achieved 61 A W^{-1} at 120 V),³⁶ our UV sensor can maintain relatively high efficiency under a low driving voltage, which is a significant advantage in areas such as flexible electronics and wearable electronics.

As control, on the other hand, ZnO QD/graphene hybrid film shows much weaker photoresponse to 370 nm light. With the same device architecture and testing method, only 820 nA increase in photocurrent is recorded at 20 V bias, corresponding to a photoresponsibility of 0.35 A W^{-1} (Fig. 6A and 6B). The weakening in UV absorption can be partly attributed to the weak absorption of ZnO QDs at 370 nm. As expected, there is no photoresponse to visible 590 nm photons for ZnO QD/graphene hybrid either (Fig. S3†). Further control experiments show that pure SDBS-graphene film has no responses to either 370 nm or 590 nm photons (Fig. 6C, 6D and Fig. S4†). Therefore, we can conclude that the majority of photogenerated current comes

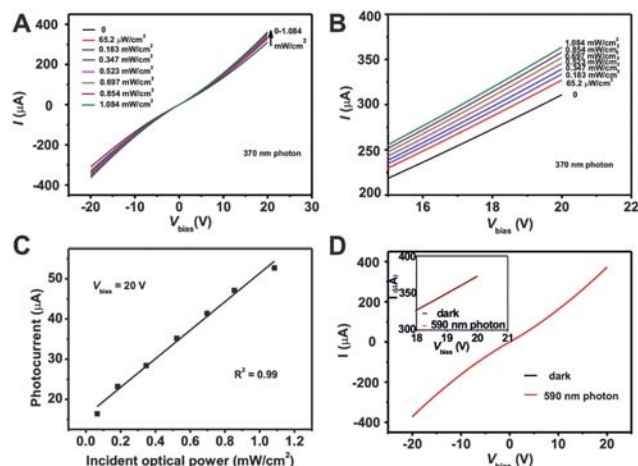


Fig. 5 (A) Current versus voltage curves for ZnO nanorod/graphene heterostructures under dark and different power 370 nm photon radiation from 0 to 1.084 mW cm^{-2} , (B) an enlarged view of (A) with V_{bias} from 15 V to 20 V, (C) photocurrent (the current increase under photon radiation) as a function of incident optical power at 20 V bias, (D) Current versus voltage curves for ZnO nanorod/graphene heterostructure under dark and $108.5 \mu\text{W cm}^{-2}$ 590 nm photon radiation. Inset: enlarged view of (D) with V_{bias} from 18 V to 20 V.

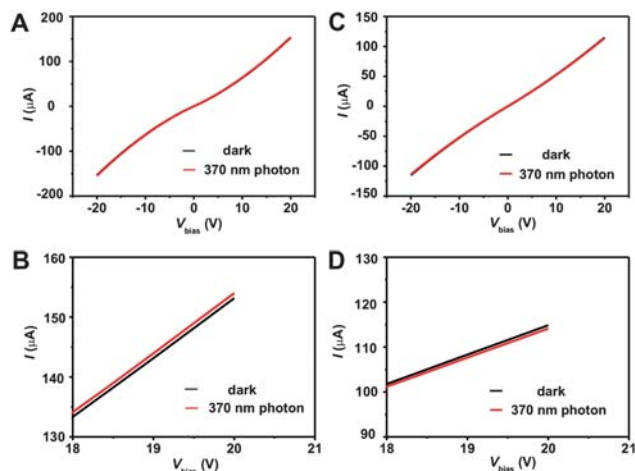


Fig. 6 Current versus voltage curves for ZnO QD/graphene hybrid (A, B) and pure SDBS-graphene (C, D) in the dark and under 1.084 mW cm^{-2} 370 nm photon radiation.

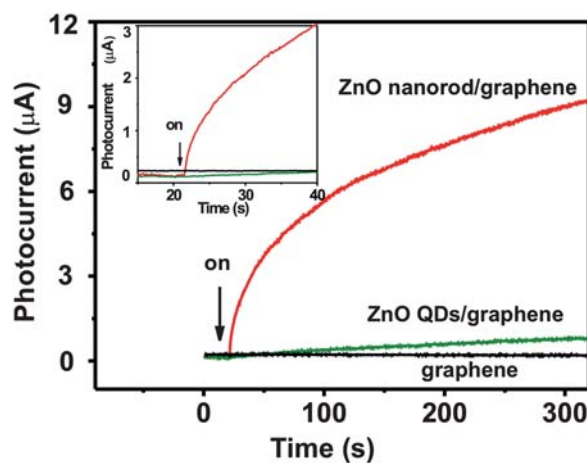


Fig. 7 Background-subtracted time-resolved photoresponses of pure SDBS-graphene, ZnO QD/graphene hybrid and the ZnO nanorod/graphene heterostructure at 1.084 mW cm^{-2} 370 nm radiation with V_{bias} of 5 V. Inset, an enlarged view of the exact starting point when light is on.

from the ZnO nanorod/graphene heterostructures, rather than ZnO QDs or SDBS-graphene.

We further investigated the kinetic behavior of photoresponses in more detail. Time-resolved photoresponses of ZnO nanorod/graphene, ZnO QD/graphene, and pure SDBS-graphene films were recorded at 5 V bias with 1.084 mW cm^{-2} power 370 nm light. Fig. 7 shows the background-subtracted time-resolve photoresponse curves of the three devices. As expected, devices with pure SDBS-graphene does not show any increase in photocurrent. A much faster photoresponse for the ZnO nanorod/graphene heterostructure is observed, compared with that of ZnO QD/graphene hybrid. Immediately after irradiation, a very steep current increase is observed for ZnO nanorod/graphene heterostructure based device, with a tangent angle of almost 90° . On the other hand, the current increase of ZnO QD/graphene based device is much more gentle. Several situations may contribute to the faster responses of ZnO nanorod/graphene heterostructure under 370 nm. First, similar to the case of *in situ* grown CdS QD/graphene heterostructure, *in situ* hydrothermal growth of ZnO nanorods on graphene will obtain better connection between ZnO nanorods and graphene than the connection between ZnO QDs and graphene formed by simple mixing.¹⁰ Second, we find the dark current of the same device increase by 50–150% after hydrothermal growth of ZnO nanorods in 90°C solution. This may be induced by further reduction and conductivity improvement of SDBS-graphene in the process of hydrothermal growth of ZnO nanorods.^{37–39} The higher electron conductivity of graphene will facilitate the photogenerated electrons transport to electrodes. Note that time-resolved

photoresponse further confirmed that there are no photocurrent generation for ZnO nanorod/graphene heterostructure, ZnO QD/graphene hybrid and pure SDBS-graphene films under 590 nm radiations (Fig. S5†).

Another aspect for the time-resolved photoresponses in ZnO nanorod/graphene heterostructure is the slow photocurrent decay after the UV light is turned off (Fig. S6†). To explore this issue, time-resolved photoluminescence (PL) of ZnO nanorod/graphene heterostructure were investigated on quartz substrate by ultrafast time-resolved emission spectroscopy experiments as we described elsewhere (Fig. 8).^{40–42} Energy gap PL emission at 385 nm was observed and it decayed dramatically in the time-resolved PL spectra from 1 to 100 ps probe time delay (Fig. 8A).⁴¹ No obvious defect emission at 450–700 nm was observed because of the high quality single crystal structure of the ZnO nanorods (Fig. 4E and 4F).⁴³ The PL decay dynamics in Fig. 8B shows that the ZnO nanorods in ZnO nanorod/graphene heterostructures (averaged time constant, 9.2 ps) have almost the same decay properties as the pure ZnO nanorods (averaged time constant, 8.5 ps), which is consistent with a previous report in the averaged time constant of ZnO nanorods.⁴¹ Previously, both we and Cao *et al.* have reported the rapid PL decay of CdS QDs in the *in situ* grown CdS QD/graphene heterostructures, compared with the pure CdS QDs. The faster decay was attributed to the large contact areas between *in situ* grown CdS QDs and graphene, and the resulting efficient quenching.^{10,19} In the present ZnO nanorod/graphene heterostructure, 500 nm to $1 \mu\text{m}$ long nanorods only contact the SDBS-graphene with one end, a very small part of the nanorods. Therefore the photogenerated carriers may be kept trapped within the ZnO for a long time before it is injected into SDBS-graphene, leading to the slow saturation in photocurrent and the slow decay in output current when the light is turned off.

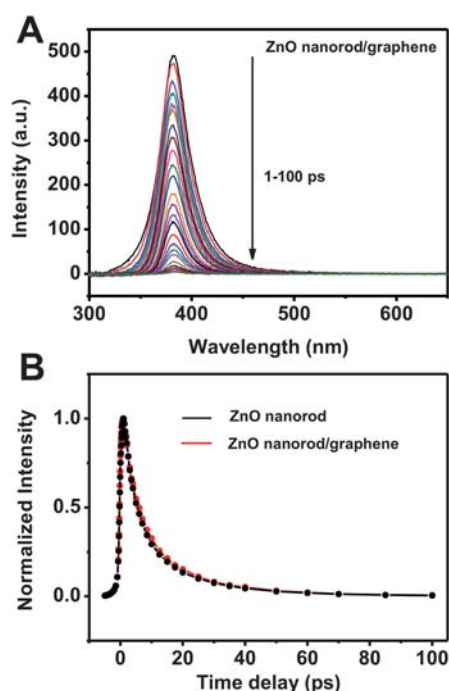


Fig. 8 (A) Time-resolved photoluminescence spectra of ZnO nanorods in ZnO nanorod/graphene heterostructure on quartz substrate with 1 to 100 ps time delay after excitation at 267 nm. (B) Photoluminescence decay at 385 nm of pure ZnO nanorods and ZnO nanorods in ZnO nanorod/graphene heterostructures on a quartz substrate.

3. Conclusions and outlook

In summary, we have demonstrated the facile synthesis of ZnO nanorod/graphene heterostructures on various substrates *via* a seeded solution growth method. Thin-film photoconductors based on ZnO nanorod/graphene heterostructure were for the first time explored as visible-blind UV sensors, which reached a photoresponsibility of 22.7 A W^{-1} at 20 V. Such a high sensitivity is attributed to the UV absorbing properties of ZnO and the high electron accepting and transporting properties of graphene. Importantly, the UV sensor had no response to visible light and can be used in UV only photodetectors. More importantly, the whole fabrication procedure was carried out in solutions and at mild temperatures. Further considering the transparent and flexible attributes of graphene, our approach should be adaptable to flexible and wearable electronic devices. Note that the prototype UV sensor was tested for 370 nm photons due to the feasibility and availability of the equipment. But according to the absorption spectrum of ZnO nanorods in Fig. S2B,† the UV sensor should have better performance to 350 nm and deeper UV light. Currently, the detection limit is $\sim 65.2 \mu\text{W cm}^{-2}$, *i.e.*, 130.4 nW taking into account the device architecture. We believe that this method can be extended for developing other photosensitive heterostructures (infrared or deep-UV) between graphene and many one-dimensional nanomaterials, for instance,

PbS, Si and GaN nanowires by choosing proper nucleation templates on graphene.

4. Experimental

Materials and chemicals

Graphite powder (325 mesh, 99.95%) and SDBS (PB, 97%) were purchased from Alfa Aesar (USA). Methanol, zinc nitrate ($\text{Zn}(\text{NO}_3)_2$), and zinc acetate ($\text{Zn}(\text{AC})_2$) were purchased from Uni-Chem Chemical Reagents with 99% purity. Hexamethylenetetramine (HMTA) (99% purity) was purchased from Sigma-Aldrich. Other reagents were purchased from Beijing Chemicals Co. Ltd. (China) with analytical grade. All reagents were used as received. Deionized (DI) water was used in all the aqueous solutions.

Synthesis of SDBS-graphene and ZnO QDs

Graphite was first oxidized to graphite oxide by Hummer method, and then exfoliated by sonication in the presence of SDBS to form graphene oxide.^{9,10,28} The graphene oxide was then chemically reduced by hydrazine to form SDBS-graphene following the method we previously published.²² In brief, 1 mg mL⁻¹ graphite oxide solution was ultrasonicated in the presence of 1–12 mg mL⁻¹ SDBS for 2 h until no obvious sediment of graphite oxide. The above exfoliated solution was chemically reduced by hydrazine at 100 °C for 12 h. The black precipitate, being SDBS-graphene, was collected by filtration followed by washing with deionized water thoroughly. ZnO QDs were synthesized following a literature procedure.²⁶ In general, 62.5 mL 0.01 M $\text{Zn}(\text{AC})_2$ methanol solution was kept at 60 °C and 32.5 mL 0.03 M NaOH was added to the solution drop by drop with strong stirring. The reaction last for over 3 h to ensure the formation of ZnO QDs.

Preparation of ZnO QD/graphene hybrid and ZnO nanorod/graphene heterostructures

175 μL 1 mg mL⁻¹ SDBS-graphene aqueous solution was added to 1 mL ZnO QDs methanol solution followed by vigorous shaking. The ZnO QD/graphene hybrid was centrifuged and washed with DI-water and methanol several times, and re-dispersed in methanol–water solution. The mixture solution of ZnO QD/graphene can form thin films by drop casting on various substrates such as silicon, glass, quartz and polyethylene terephthalate (PET). The hybrid film was further annealed at 100 °C for *ca.* 30 min to enhance its adhesion to the substrate. ZnO nanorods were then *in situ* grown from the graphene using the ZnO QD seeds. The growth of ZnO nanorod/graphene heterostructure was conducted in the 0.025 M $\text{Zn}(\text{NO}_3)_2$ and 0.025 M HMTA at 90 °C for 1 h.³⁴ To fabricate UV sensors, the thin film of ZnO QD/graphene hybrid was prepared on $\text{SiO}_2/\text{n-Si}$ substrate followed by 100 °C annealing. Then it was patterned by gold electrodes with 100 μm channel length and 2 mm width. The patterned ZnO QD/graphene hybrid thin film was placed in the solution of 0.025 M $\text{Zn}(\text{NO}_3)_2$ and 0.025 M HMTA at 90 °C for 1 h to grow ZnO nanorods.

Characterizations and measurements

The samples for AFM characterization (tapping mode) were prepared by dropping diluted SDBS-graphene solution on a Si substrate followed by gentle drying. Transmission electron microscopy (TEM) images were collected by JEM-2010 (JEOL) with accelerated voltage of 120 kV. The SEM micrographs were recorded by scanning electron microscopy (SEM) JSM-6301F (JEOL). The UV-Vis spectra were obtained from a Perkin–Elmer spectrophotometer. The experimental setup for time-resolved photoluminescence measurements was described elsewhere.^{40–42} The thin film device measurements for photonic responses were conducted in nitrogen atmosphere to exclude the influence of oxygen for the convenience of understanding the device physics. The photon irradiation was provided by 370 nm or 590 nm light-emitting diodes (LEDs). No degradation of graphene or damage of devices was found after irradiation (Fig. S7†). The electronic and optoelectronic data of the UV sensors was recorded by an Agilent 4156C Precision Semiconductor Parameter Analyzer. For ultrafast photoluminescence measurements, the samples were prepared on quartz substrates.

Acknowledgements

We thank Jinhua Li for the ZnO TEM analysis and discussion. Z.J.Z., H.X.C., and X.M.T. acknowledge The Hong Kong Polytechnic University (Project A-PJ49) for financial support of this work. Z.H.S is financially supported by the Research Grants Council (RGC) of Hong Kong, China (Project B-Q10T).

Notes and references

- 1 A. K. Geim and K. S. Novoselov, *Nat. Mater.*, 2007, **6**, 183.
- 2 Y. B. Zhang, Y. W. Tan, H. L. Stormer and P. Kim, *Nature*, 2005, **438**, 201.
- 3 S. S. Yu and W. T. Zheng, *Nanoscale*, 2010, **2**, 1069.
- 4 X. L. Li, X. R. Wang, L. Zhang, S. W. Lee and H. J. Dai, *Science*, 2008, **319**, 1229.
- 5 S. Stankovich, D. A. Dikin, G. H. B. Dommett, K. M. Kohlhaas, E. J. Zimney, E. A. Stach, R. D. Piner, S. T. Nguyen and R. S. Ruoff, *Nature*, 2006, **442**, 282.
- 6 F. Li, Y. Huang, Q. Yang, Z. Zhong, D. Li, L. Wang, S. Song and C. Fan, *Nanoscale*, 2010, **2**, 1021.
- 7 X. Wang, L. J. Zhi and K. Müllen, *Nano Lett.*, 2008, **8**, 323.
- 8 Y. Huang, X. Dong, Y. Shi, C. M. Li, L. J. Li and P. Chen, *Nanoscale*, 2010, **2**, 1485.
- 9 H. X. Chang, L. H. Tang, Y. Wang, J. H. Jiang and J. H. Li, *Anal. Chem.*, 2010, **82**, 2341.
- 10 H. X. Chang, X. J. Lv, H. Zhang and J. H. Li, *Electrochem. Commun.*, 2010, **12**, 483.
- 11 A. Reina, X. T. Jia, J. Ho, D. Nezich, H. B. Son, V. Bulovic, M. S. Dresselhaus and J. Kong, *Nano Lett.*, 2009, **9**, 30.
- 12 B. Li, X. Cao, H. G. Ong, J. W. Cheah, X. Zhou, Z. Yin, H. Li, J. Wang, F. Boey, W. Huang and H. Zhang, *Adv. Mater.*, 2010, **22**, 3058.
- 13 J. Liu, Z. Yin, X. Cao, F. Zhao, A. Ling, L. Xie, Q. L. Fan, F. Boey, H. Zhang and W. Huang, *ACS Nano*, 2010, **4**, 3987.
- 14 J. Liu, Z. Lin, T. Liu, Z. Yin, X. Zhou, S. Chen, L. Xie, F. Boey, H. Zhang and W. Huang, *Small*, 2010, **6**, 1536.
- 15 Q. He, H. G. Sudibya, Z. Yin, S. Wu, H. Li, F. Boey, W. Huang, P. Chen and H. Zhang, *ACS Nano*, 2010, **4**, 3201.
- 16 Z. Yin, S. Wu, X. Zhou, X. Huang, Q. Zhang, F. Boey and H. Zhang, *Small*, 2010, **6**, 307.
- 17 Z. J. Wang, X. Z. Zhou, J. Zhang, F. Boey and H. Zhang, *J. Phys. Chem. C*, 2009, **113**, 14071.
- 18 F. N. Xia, T. Mueller, Y. M. Lin, A. Valdes-Garcia and P. Avouris, *Nat. Nanotechnol.*, 2009, **4**, 839.

- 19 A. N. Cao, Z. Liu, S. S. Chu, M. H. Wu, Z. M. Ye, Z. W. Cai, Y. L. Chang, S. F. Wang, Q. H. Gong and Y. F. Liu, *Adv. Mater.*, 2010, **22**, 103.
- 20 X. M. Geng, L. Niu, Z. Y. Xing, R. S. Song, G. T. Liu, M. T. Sun, G. S. Cheng, H. J. Zhong, Z. H. Liu, Z. J. Zhang, L. F. Sun, H. X. Xu, L. Lu and L. W. Liu, *Adv. Mater.*, 2010, **22**, 638.
- 21 E. Munoz, E. Monroy, J. L. Pau, F. Calle, F. Omnes and P. Gibart, *J. Phys.: Condens. Matter*, 2001, **13**, 7115.
- 22 S. Liang, H. Sheng, Y. Liu, Z. Huo, Y. Lu and H. Shen, *J. Cryst. Growth*, 2001, **225**, 110.
- 23 H. Kind, H. Q. Yan, B. Messer, M. Law and P. D. Yang, *Adv. Mater.*, 2002, **14**, 158.
- 24 Z. L. Wang and J. H. Song, *Science*, 2006, **312**, 242.
- 25 B. Weintraub, Z. Zhou, Y. Li and Y. Deng, *Nanoscale*, 2010, **2**, 1573.
- 26 J. B. Baxter and E. S. Aydil, *Appl. Phys. Lett.*, 2005, **86**, 053114.
- 27 Q. H. Li, T. Gao, Y. G. Wang and T. H. Wang, *Appl. Phys. Lett.*, 2005, **86**, 123117.
- 28 H. X. Chang, G. F. Wang, A. Yang, X. M. Tao, X. Q. Liu, Y. D. Shen and Z. J. Zheng, *Adv. Funct. Mater.*, 2010, **20**, 2893.
- 29 Y. Hernandez, V. Nicolosi, M. Lotya, F. M. Blighe, Z. Y. Sun, S. De, I. T. McGovern, B. Holland, M. Byrne, Y. K. Gun'ko, J. J. Boland, P. Niraj, G. Duesberg, S. Krishnamurthy, R. Goodhue, J. Hutchison, V. Scardaci, A. C. Ferrari and J. N. Coleman, *Nat. Nanotechnol.*, 2008, **3**, 563.
- 30 D. Li, M. B. Müller, S. Gilje, R. B. Kaner and G. G. Wallace, *Nat. Nanotechnol.*, 2008, **3**, 101.
- 31 X. Y. Qi, K. Y. Pu, X. Z. Zhou, H. Li, B. Liu, F. Boey, W. Huang and H. Zhang, *Small*, 2010, **6**, 663.
- 32 C. Pacholski, A. Kornowski and H. Weller, *Angew. Chem., Int. Ed.*, 2002, **41**, 1188.
- 33 H. M. Xiong, Y. Xu, O. G. Ren and Y. Y. Xia, *J. Am. Chem. Soc.*, 2008, **130**, 7522.
- 34 L. Vayssieres, *Adv. Mater.*, 2003, **15**, 464.
- 35 J. H. He, J. H. Hsu, C. W. Wang, H. N. Lin, L. J. Chen and Z. L. Wang, *J. Phys. Chem. B*, 2006, **110**, 50.
- 36 Y. Z. Jin, J. P. Wang, B. Q. Sun, J. C. Blakesley and N. C. Greenham, *Nano Lett.*, 2008, **8**, 1649.
- 37 Y. Zhou, Q. L. Bao, L. A. L. Tang, Y. L. Zhong and K. P. Loh, *Chem. Mater.*, 2009, **21**, 2950.
- 38 H. Zhang, X. J. Lv, Y. M. Li, Y. Wang and J. H. Li, *ACS Nano*, 2010, **4**, 380.
- 39 P. V. Kamat, *J. Phys. Chem. Lett.*, 2010, **1**, 520.
- 40 W. M. Kwok, C. S. Ma and D. L. Phillips, *J. Am. Chem. Soc.*, 2006, **128**, 11894.
- 41 W. M. Kwok, A. B. Djuricic, Y. H. Leung, W. K. Chan and D. L. Phillips, *Appl. Phys. Lett.*, 2005, **87**, 223111.
- 42 W. M. Kwok, C. S. Ma and D. L. Phillips, *J. Phys. Chem. B*, 2009, **113**, 11527.
- 43 L. E. Greene, M. Law, J. Goldberger, F. Kim, J. C. Johnson, Y. F. Zhang, R. J. Saykally and P. D. Yang, *Angew. Chem., Int. Ed.*, 2003, **42**, 3031.